

Theoretical and experimental investigation of the near field under ordered silica spheres on substrate

S.M. Huang · Z.A. Wang · Z. Sun · Z.B. Wang · Boris Luk'yanchuk

Received: 10 February 2009 / Accepted: 4 May 2009 / Published online: 23 May 2009
© Springer-Verlag 2009

Abstract Investigation on the optical resonance and near field effects of a 2D periodic dielectric spheres on metallic surfaces by combining theoretical calculations with experimental studies were carried out. The light scattering and coupling was numerically studied. Nanostructures were fabricated on the metallic surfaces using these arrays of micro- and nano-spheres with a single laser pulse (KrF, $\lambda = 248$ nm). The occurrence of such nanostructures is well explained by the theoretical calculations. The results can be useful in investigation and development of spheres-assisted nano-patterning.

PACS 81.16.Mk · 61.80.Ba · 81.16.Rf · 81.65.Cf

1 Introduction

The development of near-field optics and photonics has opened a door to spatially-controlling matter on a nanometer

scale [1]. A variety of nanofabrication techniques employing optical near fields has been developed as a new technology to overcome the diffraction limit [2–15]. We have reported a method to use regular two-dimensional (2D) periodic lattices of micro- or nano-spheres for a single-step parallel surface patterning to generate hexagonal arrays of 2D holes, nanobumps and nanoparticles [11–15]. This nanofabrication method is based on the optical near-field under transparent or half transparent small sized spheres ranging from several tens of nanometer to several tens of micrometers. The method is a high-speed parallel processing technique which permits single-step production of millions of holes/cones/nanoparticles with long-range order on the surface using a single or a few laser shots. In this nanofabrication, the calculation of the near field of ensembles of micro or nano- spheres on substrates is a fundamental theoretical issue. However, most of previous theoretical investigations were generally carried out based on the single particle models, e.g. Mie theory [16] or a single particle-on-surface theory [10–17], in which the field interactions and coupling between the neighbouring particles have not been well explored. Until recently, several theoretical attempts have been made to analyze the near field optics of a 2D periodic system on a substrate [18–22].

The analytical solution of the light scattering of aggregates can be obtained by the generalized Mie theory [23, 24], which uses either *T*-matrix method [23] or the order-of-scattering method [24]. Nevertheless exact analytic solution of this problem is surprisingly difficult. Numerical calculation methods for solving electromagnetic problems for an arbitrary geometry, such as the multiple multi-pole (MMP) technique [25], the Green's function method [26], the finite difference time domain (FDTD) technique [27] and Finite Integral Technique (FIT) [28] have been developed. These numerical methods have also been applied to

S.M. Huang (✉) · Z.A. Wang · Z. Sun
Engineering Research Center for Nanophotonics and Advanced Instrument, Ministry of Education, Department of physics, East China Normal University, North Zhongshan Rd. 3663, Shanghai 200062, P.R. China
e-mail: smhuang@phy.ecnu.edu.cn

Z.B. Wang
Laser Processing Research Centre, School of Mechanical, Aerospace and Civil Engineering, University of Manchester, Sackville Street, Manchester, M60 1QD, UK

B. Luk'yanchuk
Data Storage Institute, DSI Building, 5 Engineering Drive 1, Singapore 117608, Republic of Singapore

solving problems in near-field optics. Recently, the optical transmission through metal or silicon coated monolayers of microspheres and the field distribution in these monolayers were calculated by FDTD modeling [19–21]. Moreover, a commercial FIT software package (CST Microwave Studio 2006) was used for solving electromagnetic problems of transparent particle chains situated in a homogeneous medium with Cartesian grids system (FDTD module) [29]. The field interactions between the neighbouring particles were explored.

In this paper, we report the results of detailed investigation on the optical resonance and near field effects of a 2D periodic dielectric spheres on metallic surfaces by combining theoretical calculations with experimental studies. We present nanostructures fabricated on metallic surfaces using the regular 2D arrays by a single pulsed laser irradiation (KrF, $\lambda = 248$ nm). The morphologies of the created nanostructures were characterized by an atomic force microscope (AFM) and a scanning electron microscope (SEM). Calculations of the field distribution of 2D periodic spheres on the substrate surface were presented. Good agreement between theoretical calculations and experimental results has been observed.

2 Theoretical calculations and experimental details

CST Microwave Studio 2006 is a general purpose and full 3D microwave modeling platform that incorporates eigenmode, frequency and time-domain solvers for various applications [30]. The electromagnetic field distribution in the systems of hexagonally closed-packed colloidal monolayers on metallic surfaces was simulated by using this software. Spheres with diameters in the range of 140 nm to 1000 nm were studied. These particles are transparent to the ultraviolet (UV) light. Upon choosing a suitably refined computational grid (the maximum grid length was chosen as wavelength/10 in the paper), the corresponding numerical solution gives an accurate representation of the dynamics of the electromagnetic field.

Figure 1 shows a system of 19-spheres with a diameter of $2a$ on a bulk Al, where a is the radius of the nonabsorptive sphere. This system was studied theoretically in this paper. The 19-particles are arranged in the xy plane to form a close-packed triangular lattice with an interparticle spacing $d = 2$ nm. The origin of the coordinates is taken at the center of the middle sphere. The xy plane is set parallel to the surface of the substrate and the x axis goes through the centers of the spheres. The substrate is situated in the positive z region. There is a separation distance along the z -axis ($g = 2$ nm) between the spheres and the Al surface. Let the plane-wave electromagnetic field of wave vector k be incident from the top of the sphere array ($z < 0$). The

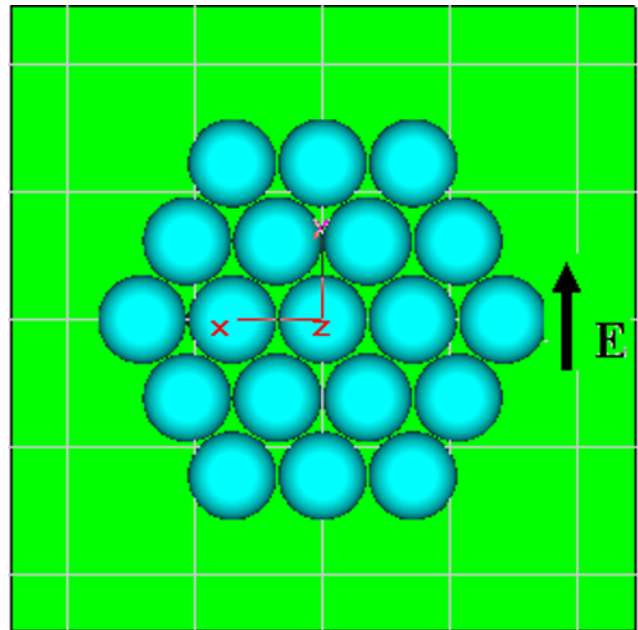


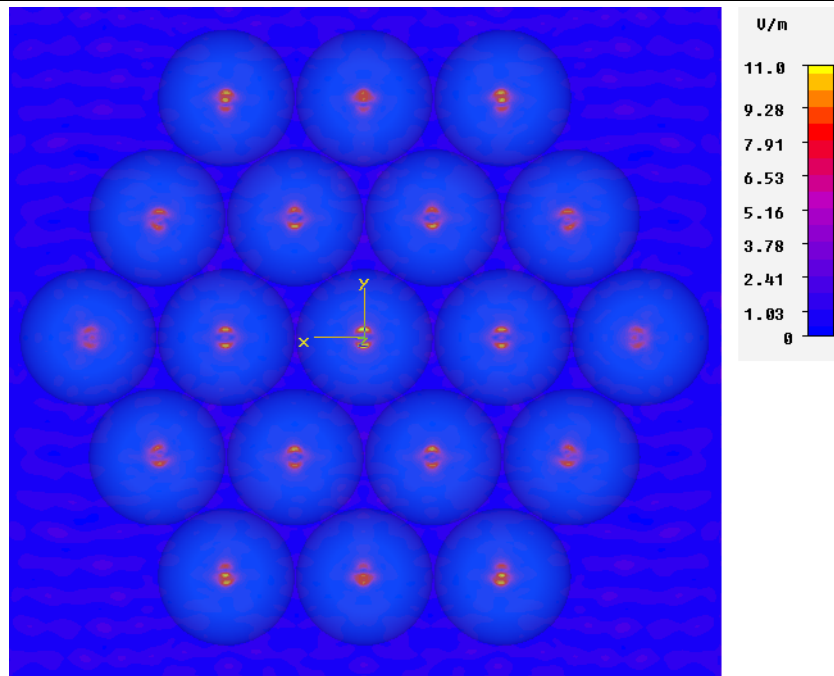
Fig. 1 Schematic of 19-spheres -Al sample system simulated

wave propagates along the z coordinate, the electric vector is along the y coordinate, and the magnetic vector along the $-x$ coordinate. The top surface of the bulk Al is at $z = a + g$. The Transient Solver module of the CST software was used for this work. This module is a general purpose module of the 3D EM simulator [30]. We set the accuracy in the Solver Parameters menu at a setting of -50 dB which means the transient solver stops at the moment when the remaining energy of the time signals within the calculation domain decays to 10^{-5} compared to the maximum energy. The computational domain is rectangular with dimensions $-8a \leq x \leq 8a$, $-8a \leq y \leq 8a$ and $4a \leq z \leq 4a$. A perfectly matched layer (PML) open boundary conditions were applied for all the boundaries of the computational domain (numerical reflection coefficient $< 0.01\%$ with the typical four-layered PML).

In the next section, theoretical studies of the light interaction within monolayer spheres on Al surface are presented. In all modeling, the spheres were considered uniform in size with a diameter in the range of 140 nm to 1000 nm. The refractive index of spheres at 248 nm was taken to be 1.51. The value was directly taken from the bulk SiO₂ experimental data in Palik's book [31]. It means that we are not including nonlocal or size dependent dielectric response for small particles. To make this effect negligible, we have limited particle diameter to be not smaller than 140 nm in our simulations. Meanwhile, we limited our investigation on particles in spherical shape. The permittivity of Al at 248 nm is described by the Drude model:

$$\varepsilon(\omega) = \varepsilon_{\infty} - \frac{\omega_p^2}{\omega(\omega - i\nu_c)}$$

Fig. 2 Electric field amplitude $|E|$ enhancement distribution under 19-spheres on the Al top surface. The size of all spheres is 950 nm in diameter



where the high-frequency bulk permittivity $\epsilon_\infty = 1$, the bulk plasmon frequency $\omega_p = 3.028 \times 10^{15}$ Hz, and the electron collision frequency $\nu_c = 1.318 \times 10^{13}$ Hz. These parameters are obtained by fitting the model to the experimental data in the visible and ultraviolet range taken from the literature [32].

Hexagonally closed-packed colloidal monolayers can be directly prepared on the surface by a spin-coating or a self-organizing process. The relevant techniques have been described in detail in [33, 34]. In the preparation of our samples, aluminum films (200 nm in thickness) on silicon substrates were used as samples for particle assembling. These Al films were deposited by the sputtering method. Spheres were applied to the samples after the particle suspension had been diluted with deionized (DI) water. Isolated spheres were deposited onto the substrate by controlled application of a colloidal suspension with desired concentration. The light source was a KrF excimer laser with a wavelength of 248 nm and pulse width of 23 ns. The laser fluence used was about 300 mJ/cm². The 25 mm \times 5 mm rectangular laser spot had a uniform light intensity. Compared with the other lasers such as femtosecond lasers, excimer lasers have a larger beam size. The laser beam was incident normally on the sample with particles on the surface. Each sample was treated using a single laser pulse. The surfaces before and after laser treatment were examined with a high-resolution optical microscope. During the laser irradiation, it was found that most of particles were removed from the sample surface. The sample was further ultrasonically cleaned before AFM and SEM measurements were done.

3 Results and discussion

Figure 2 shows the calculated local amplitude enhancement distribution of the electric field, $|E|$, in Al and on the top surface of the bulk Al under 19-spheres. The diameter of the sphere is 950 nm. The x - y region under each sphere and the circumferences of the spheres on the Al surface can be seen clearly from the shadows shown in Fig. 2. From the figure, the electric field is enhanced and localized under each sphere in the system of 19-spheres on the substrate. There are three peaks in the field distribution within the x - y region under each sphere on the Al surface. The peak value under the sphere center is much smaller than those of the other two peaks along a direction parallel to the y axis. The two small brightest spots under each sphere in Fig. 2 are mainly due to the y component of the electric field. The calculated local amplitude $|E|$ enhancement distribution of an isolated sphere on the Al surface is presented in Fig. 3. From this figure, the field under the isolated sphere gives a bright spot and shows a Gaussian distribution, similar to that calculated by the Mathematica program based on a single particle-on-surface theory [11, 35].

Figure 4 shows the characteristics of the local $|E|$ enhancement crossing the center of the Al surface at $z = 477$ nm, $x = 0$ and -1000 nm $\leq y \leq 1000$ nm for both an isolated sphere and 19-sphere systems. The peak value under the isolated sphere is about 8, similar to that of the middle and small peak (a value of 6) for the multi-sphere system shown in Fig. 4. However, for the latter, there are another two strong peaks with a value of ~ 11 under each sphere and along a direction parallel to the y axis. It is remarkable that the local-field intensity is as large as 11^2 . This type

Fig. 3 Electric field amplitude $|E|$ enhancement distribution under an isolated sphere on the Al top surface. The size of all spheres is 950 nm in diameter

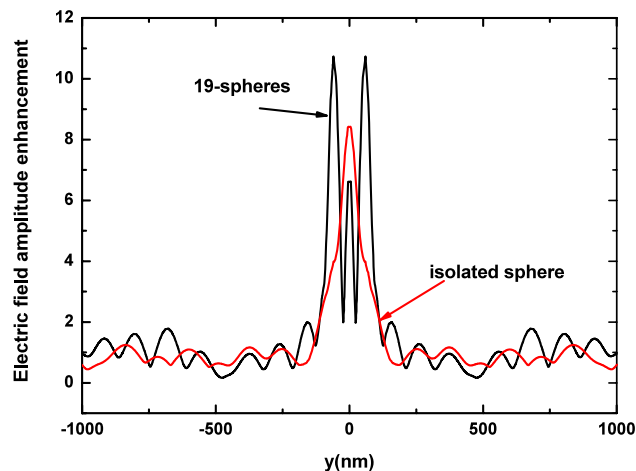
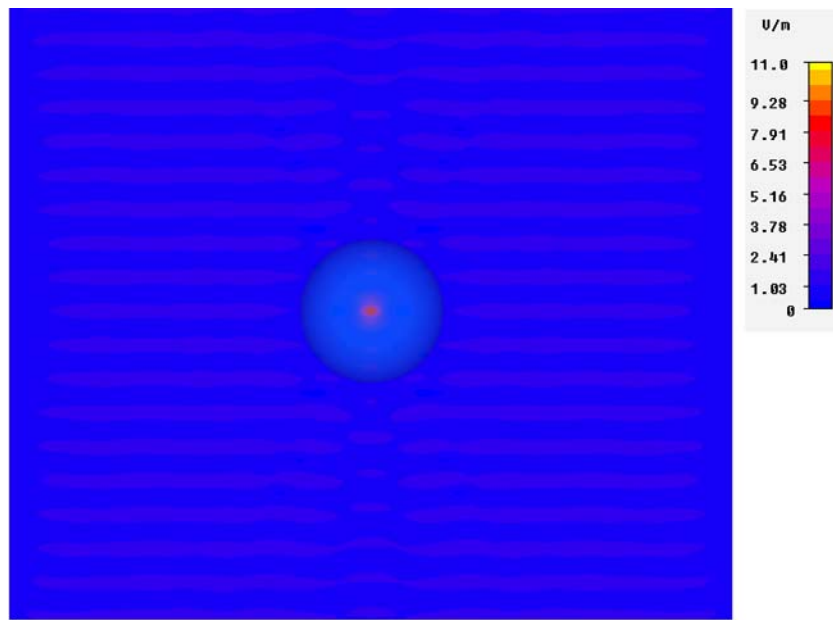


Fig. 4 Electric field amplitude $|E|$ enhancement distribution along the y axis under the centered sphere on the Al surface for both an isolated sphere and 19-sphere systems. The size of all spheres is 950 nm in diameter

of large enhancement is similar to the values obtained for 3D lattice of spheres in [36]. By comparing the CST simulation results for both isolated and multi-sphere systems shown in Figs. 2–4, the inter-sphere coupling seems strongly driven by the polarization of the incident light. Xu H.X. [24] calculated the near field of 3-Ag particle system and found the interparticle coupling also showed incident polarization sensitivity. Moreover, from Fig. 4, for both isolated and multi-spheres, the light energy is localized and confined in the small x – y regions under the spheres. However, the dimensions of the localized and confined regions are different. The full width at half maximum (FWHM) of the electric field amplitude enhancement for the former system is 80 nm,

while the FWHM of the enhancement is wider and with a value of 190 nm for the latter system due to the coupling between the neighboring particles.

Figure 5 shows the calculated local amplitude enhancement distribution of the electric field, $|E|$, in Al and on the Al top surface under 19-SiO₂ spheres with a radius $a = 70$ nm. From Fig. 5, the electric field is still enhanced and localized at contact points between the spheres and the substrate due to spherical confinement and multiple scattering in the system. However, the shape of the electric field $|E|$ distribution is considerably different from that for the big sphere ($a = 475$ nm) array system shown in Fig. 2. Four big brightest spots with a peak $|E|$ value of ~ 4 appear at four contact points between the spheres and the substrate, while the contours under three spheres at or near the center of the surface and along the x axis look like three lemniscates. The electric field enhancement weakens and the size of the brightest spot becomes smaller under the outer spheres. Therefore, the near field image of scattered radiation in the 19-small sphere system has a marked anisotropic character.

In experiments spheres were arranged in hexagonal close-packed monolayers. The quality of the monolayer over a large surface area depends on many factors such as surface roughness, wettability, solution concentration, the particle size and temperature. For micrometer or bigger spheres, a high quality monolayer with long-range order can be easily obtained on the substrate by a spin-coating or a self-organizing process. Figure 6 shows an optical image of 950 nm SiO₂ particle array on an Al surface before laser irradiation. Spheres were periodically arranged in hexagonal form with quite long-range order. However, for the sub-micron spheres, it is very difficult to obtain high quality

Fig. 5 Electric field amplitude $|E|$ enhancement distribution under 19-spheres on the Al top surface. The size of all spheres is 140 nm in diameter

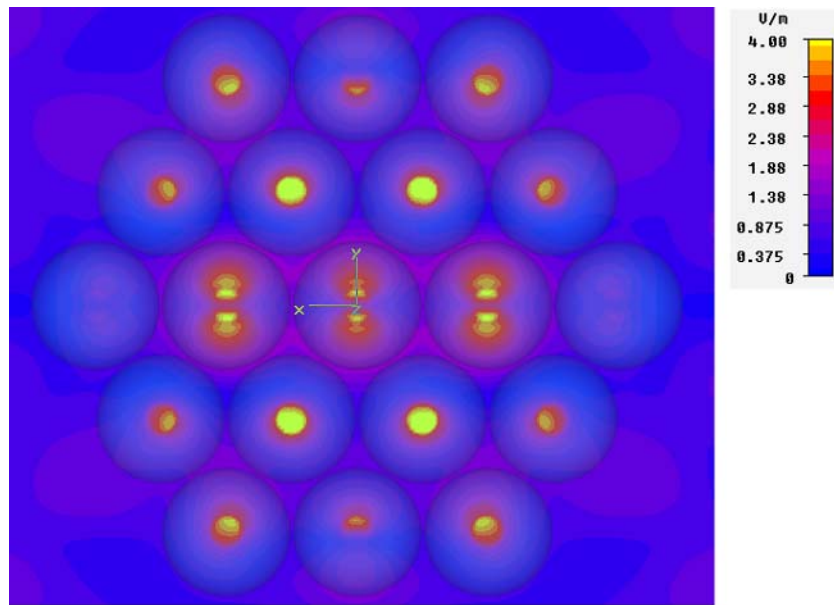
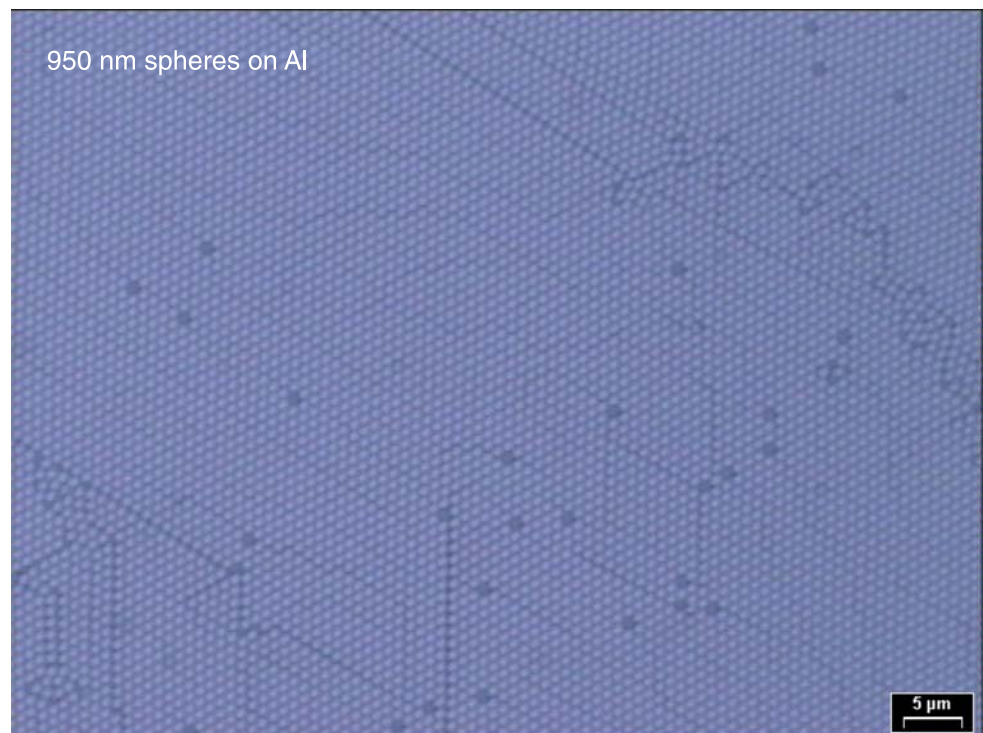


Fig. 6 Optical image of monolayer of 950 nm spheres on an Al surface before laser irradiation

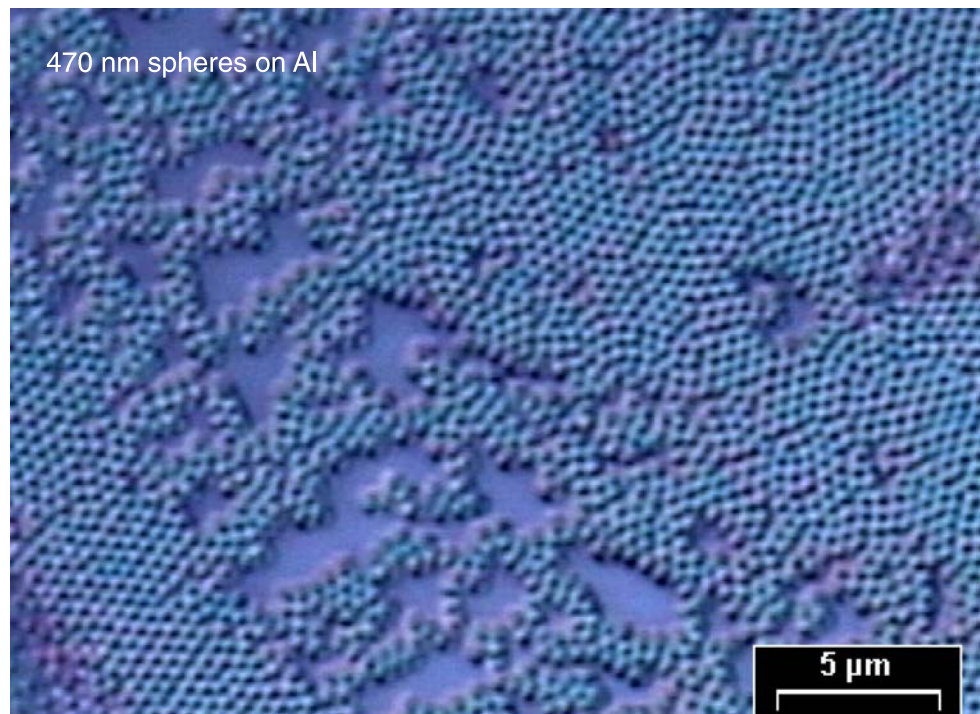


monolayer with long-range order. Figure 7 shows an optical image of 470 nm SiO_2 particle array on an Al surface without laser treatment. From the figure, the monolayer was generally observed as a multi-domain arrangement. At the edge regions of the regular arrays which were with short-range orders, particles were arranged in a random and dispersive form. When the spheres were even smaller, regular arrays of smaller number of particles in hexagonal form were often obtained on the substrate. Therefore, our calculation based

on the system of 19-spheres on substrate can be expected to address and explain the nanofabrication results introduced in the following sections.

The first laser treated sample is with 950 nm silica spheres on the Al surface. Figure 8(a) shows a typical SEM morphology of a periodic pit array formed after laser irradiation. The periodic pit array reflects the previous positions of the colloid spheres on the surface shown in Fig. 6. With higher magnification, clearer morphologies and fea-

Fig. 7 Optical image of monolayer of 470 nm spheres on an Al surface before laser irradiation

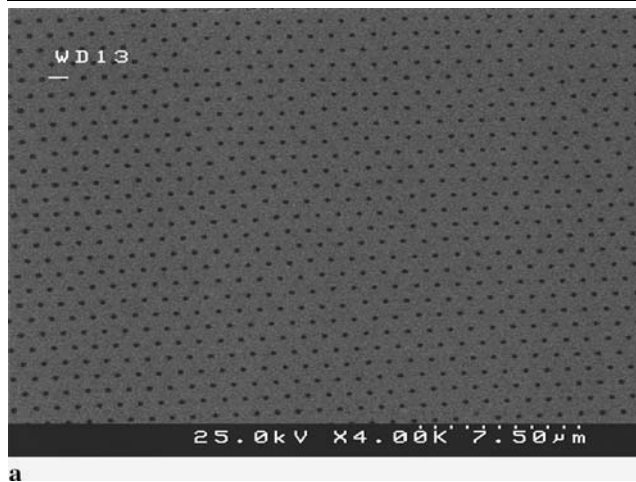


tures of the created patterns under spheres can be observed in Fig. 8(b). There is a hole in the middle of each created pattern. The depth and the diameter of the hole are about 3 nm and 200 nm respectively. The lateral size of the formed holes is very close to the FWHM of the electric field amplitude enhancement due to the coupling between the neighboring particles as shown in Figs. 2 and 4. By comparing the theoretical and experimental results shown Figs. 2 and 8, respectively, we can see that the morphologies and the features of the created hexagonal patterns on the Al surface are very similar to the simulated near field or the optical resonance images under spheres.

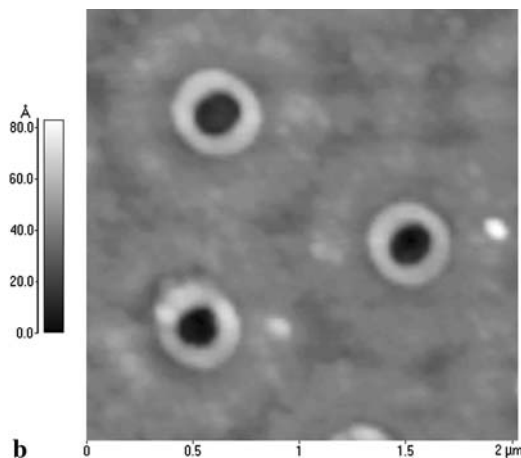
PS particles with a size of 140 nm in diameter were applied to the second sample. After laser treatment by a single pulse, holes were created on an Al surface and shown in Fig. 9. The created holes at the different contact points between the spheres and the substrate in a hexagonal array have quite different depths from 1.6 nm to 3.5 nm and diameters from 20 nm to 31 nm. These results may be attributed to the anisotropic character of the near field under spheres with a radius of 70 nm as shown in Fig. 5. The four bigger and deeper holes in Fig. 9 could be correspondingly attributed to the four bigger brightest spots shown in Fig. 5.

In the above multi-sphere systems, the electric field amplitude enhancements correspond to the excitation of eigenstates of the system. The eigenstates of the whole system are approximately given by the linear combination of those of the monolayer and the substrate. When eigenstates are excited with laser irradiation, there occurs the enhancement of near field due to large evanescent components of diffracted

light. As a result, the electric field is localized near the system. Currently, high-precision microspheres (size variation <5%) of different sizes and materials are commercially available at low cost. 2D photonic crystals (PC) with long-range order, such as a monolayer of periodically arrayed dielectric spheres on a substrate can be easily fabricated. Many theoretical [18] and experimental [37] studies have been focused on the transmission spectra and photonic band structures of such PC's. A slablike PC is different from ordinary 2D PC's composed of infinitely long parallel cylinders, in that it has a finite thickness in one direction. Consequently, there is energy dissipation in that direction, which gives rise to a finite lifetime of its eigenstates. There is also a significant enhancement of the electric field near the surface (near field) by diffracted evanescent waves due to the 2D periodicity [18]. This enhancement can be observed by the use of a scanning near-field optical microscope (NSOM) [38]. But, NSOM is a very expensive facility. Its availability is limited. Due to the limitation of NSOM, reports in combination of theoretical calculations with experimental studies in this area are very scarce. Our work together with other groups' [19–22] provided a simple and cheap method to examine and observe the near field enhancement by diffracted evanescent waves due to the 2D periodicity. By using this method, we demonstrated the agreement between experiment and theory for photonic crystals of spheres in the UV region. Our results will be useful for the development of new photon technologies such as laser manipulation of atoms, enhanced Raman scattering, high density data storage, displays, light-emitting diodes and sensors.



a



b

Fig. 8 (a) and (b) SEM and AFM images of periodic pit arrays formed after illumination of isolated 950 nm spheres on an Al surface by a single pulse with a laser fluence of 300 mJ/cm^2

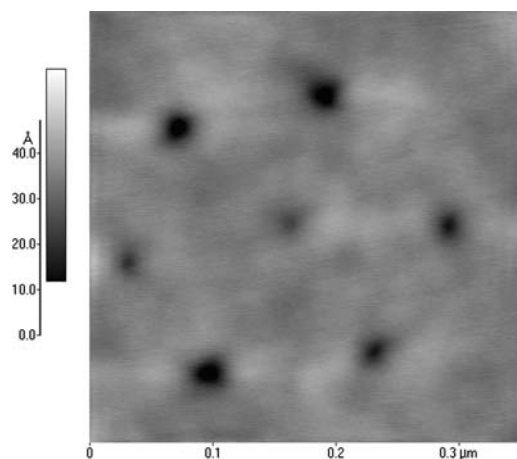


Fig. 9 AFM image of pits formed after illumination of isolated 140 nm spheres on an Al surface by a single pulse with a laser fluence of 300 mJ/cm^2

4 Conclusions

The combination of theoretical calculations with experimental studies provides an accurate description of the light scattering and near field interaction in particle hexagonal-array systems on metallic surfaces. This fundamental knowledge is critical to assess the single-step parallel surface patterning technology and will significantly contribute to the development and applications of the new photon technology. In this paper, the light scattering and coupling in the particle array systems was numerically studied. Nanostructures were fabricated on metallic surfaces using these particle arrays by the single laser pulse. A consistency between the experimental and theoretical results has been observed.

Acknowledgements This work was supported by National Natural Science Foundation of China (No. 10774046), Shanghai Municipal Science & Technology Committee (No. 0852nm06100, No. 08230705400) and Program for Changjiang Scholars and Innovative Research Team in University.

References

1. M. Ohtsu, H. Hori, *Near-Field Nano-optics* (Kluwer Academic, Dordrecht, 1999)
2. E. Betzig, J.K. Trautman, *Science* **257**, 189 (1992)
3. H. Schmid, H. Biebuyck, B. Michel, *Appl. Phys. Lett.* **72**, 2379 (1998)
4. M.M. Alkaisi, R.J. Blaikie, S.J. McNab, R. Cheung, D.R.S. Cumming, *Appl. Phys. Lett.* **75**, 3560 (1999)
5. J.G. Goodberlet, *Appl. Phys. Lett.* **76**, 667 (2000)
6. A.A. Gorbunov, W. Pompe, *Phys. Status Solidi A* **145**, 333 (1994)
7. Y.F. Lu, Z.H. Mai, G. Qiu, W.K. Chim, *Appl. Phys. Lett.* **75**, 2359 (1999)
8. S.M. Huang, M.H. Hong, Y.F. Lu, B.S. Luk'yanchuk, W.D. Song, T.C. Chong, *J. Appl. Phys.* **91**, 3268 (2002)
9. S.M. Huang, M.H. Hong, Y.F. Lu, B.S. Luk'yanchuk, W.D. Song, T.C. Chong, *J. Vac. Sci. Technol. B* **20**(3), 1118 (2002)
10. M. Mosbacher, H.-J. Münzer, J. Zimmermann, J. Solis, J. Boneberg, P. Leiderer, *Appl. Phys. A* **72**, 41 (2001)
11. S.M. Huang, M.H. Hong, B.S. Luk'yanchuk, Y.W. Zheng, W.D. Song, Y.F. Lu, T.C. Chong, *J. Appl. Phys.* **92**, 2495 (2002)
12. S.M. Huang, B.S. Luk'yanchuk, M.H. Hong, T.C. Chong, *Appl. Phys. Lett.* **82**, 4809–4811 (2003)
13. S.M. Huang, M.H. Hong, B.S. Luk'yanchuk, T.C. Chong, *Appl. Phys. A* **77**, 293–296 (2003)
14. S.M. Huang, Z. Sun, B.S. Luk'yanchuk, M.H. Hong, L.P. Shi, *Appl. Phys. Lett.* **86**, 161911 (2005)
15. S.M. Huang, Z. Sun, Y.F. Lu, *Nanotechnology* **18**, 025302 (2007)
16. G. Mie, *Ann. Phys.* **25**, 377 (1908)
17. P.A. Bobbert, J. Vliet, *Physica* **137A**, 209 (1986)
18. Y. Kurokawa, H. Miyazaki, Y. Jimba, *Phys. Rev. B* **69**, 155117 (2004)
19. L. Landström, N. Arnold, D. Brodoceanu, K. Piglmayer, D. Bäuerle, *Appl. Phys. A* **83**(2), 271–275 (2006)
20. N. Arnold, *Appl. Phys. A* **92**(4), 1005–1012 (2008)
21. L. Landström, D. Brodoceanu, D. Bäuerle, F.J. Garcia-Vidal, S.G. Rodrigo, L. Martin-Moreno, *Optics Express* **17**, 761–772 (2009)
22. A. Pikulin, N. Bityurin, G. Langer, D. Brodoceanu, D. Bäuerle, *Appl. Phys. Lett.* **91**(19), 191106 (2007)

23. J.H. Bruning, Y.T. Lo, IEEE Trans. Antennas Propag. **AP-19**, 378 (1971)
24. H.X. Xu, Phys. Lett. A **321**, 411 (2003)
25. C. Hafner, *The Generalized Multiple Multipole Technique for Computational Electromagnetics* (Artech House, Norwood, 1990)
26. O.J.F. Martin, C. Girard, A. Dereux, Phys. Rev. Lett. **74**, 526 (1995)
27. A. Taflové (ed.), *Computational Electrodynamics: The Finite-Difference Time-Domain Method*, 3rd edn. (Artech House, Norwood, 2005)
28. T. Weiland, Int. J. Numer. Model. **9**, 295 (1996)
29. Z.B. Wang, B.S. Luk'yanchuk, W. Guo, S.P. Edwardson, D.J. Whitehead, L. Li, Z. Liu, K.G. Watkins, J. Chem. Phys. **128**, 094705 (2008)
30. Available at: <http://www.cst.com>
31. E.D. Palik, *Handbook of Optical Constants of Solids* (Academic, San Diego, 1985)
32. M. Markovic, A.D. Rakic, Appl. Opt. **29**, 3479 (1990)
33. M. Mosbacher, N. Chaoui, J. Siegel, V. Dobler, J. Solis, J. Boneberg, C.N. Afonso, P. Leiderer, Appl. Phys. A **69**, S331 (1999)
34. F. Burmeister, C. Schäfle, B. Keilhofer, C. Bechinger, J. Boneberg, P. Leiderer, Adv. Mater. **10**, 495 (1998)
35. B.S. Luk'yanchuk, Y.W. Zheng, Y.F. Lu, Proc. SPIE **4065**, 576 (2000)
36. K. Ohtaka, Y. Tanabe, J. Phys. Soc. Jpn. **65**, 2670 (1996)
37. H.T. Miyazaki, H. Miyazaki, K. Ohtaka, T. Sato, J. Appl. Phys. **87**, 7152 (2000)
38. T. Fujimura, T. Itoh, A. Imada, R. Shimada, T. Koda, N. Chiba, H. Muramatsu, H. Miyazaki, K. Ohtaka, J. Lumin. **87–89**, 954 (2000)